POLITECNICO DI TORINO
Repository ISTITUZIONALE

Understanding XR Device Dynamics: A Measurement-based Model for QoE-aware Design

Original
Understanding XR Device Dynamics: A Measurement-based Model for QoE-aware Design / Chukhno, O., Mario Zappalà, D., Malandrino, F., Catania, A., Chiasserini, C.F., Molinaro, A.. - (2026). (IEEE GLOBECOM 2026 Macao (Chi) 7 - 11 December 2026).

Availability:
This version is available at: 11583/3013820 since: 2026-08-01T09:19:24Z

Publisher:
IEEE

Published
DOI:

Terms of use:

This article is made available under terms and conditions as specified in the corresponding bibliographic description in the repository

Publisher copyright
IEEE postprint/Author's Accepted Manuscript

©2026 IEEE. Personal use of this material is permitted. Permission from IEEE must be obtained for all other uses, in any current or future media, including reprinting/republishing this material for advertising or promotional purposes, creating new collecting works, for resale or lists, or reuse of any copyrighted component of this work in other works.

(Article begins on next page)

19 November 2026

Understanding XR Device Dynamics: A Measurement-based Model for QoE-aware Design

Olga Chukhno*, Domenico Mario Zappalà*, Francesco Malandrino†, Alessandro Catania‡, Carla Fabiana Chiasserini§, and Antonella Molinaro*
*University Mediterranea of Reggio Calabria, Italy and CNIT, Italy, †National Research Council of Italy (CNR-IEIIT), Italy
‡University of Pisa, Italy, § Politecnico di Torino, Italy, CNIT, Italy, and Chalmers University of Technology, Sweden
e-mail: {*olga.chukhno,domenico.zappala,antonella.molinaro*}*@unirc.it,*
francesco.malandrino@cnr.it,alessandro.catania@unipi.it,carla.chiasserini@polito.it.

***Abstract*—Extended Reality (XR) applications are highly sensitive to device-level constraints, where power consumption, battery depletion, and thermal dynamics directly impact the Quality of Experience (QoE) perceived by users. In this paper, we present a comprehensive study of XR devices operating under realistic conditions, focusing on the interplay among workload, energy consumption, and thermal behavior. Building on an extensive experimental campaign conducted under diverse operating and ambient conditions, we propose a compact linear model that captures the joint evolution of power consumption, battery dynamics, and device temperature. Our results show that the proposed model provides an accurate yet tractable representation of device dynamics, enabling the prediction of performance degradation phenomena that directly affect QoE in XR applications. Furthermore, the model helps identify the key factors limiting system sustainability and provides insights for QoE-aware XR system design. Our dataset will be made publicly available on Zenodo upon acceptance of the paper.**

***Index Terms*—XR, QoE, AR/VR, thermal dynamics, battery consumption, predictive models, measurement-based modeling.**

I. Introduction and Motivation

Extended reality (XR) is one of the most demanding application domains for next-generation networks, where stringent system constraints directly impact the Quality of Experience (QoE) perceived by users [1]. A major challenge of XR systems stems from the mismatch between the high computational requirements of XR services – which involve complex tasks such as rendering virtual environments, processing sensor data, and generating personalized content, as well as executing machine learning (ML) inference tasks such as object recognition [2] – and the stringent hardware constraints of wearable XR devices [3]. This mismatch not only challenges system design but also directly degrades QoE, e.g., through increased latency or thermally induced performance throttling.

Advanced radio access network (RAN) technologies enable XR applications by providing the connectivity and computational support for increasingly complex and artificial intelligence (AI)-driven workloads. However, recent measurement studies have demonstrated that infrastructure evolution and operational updates significantly affect traffic patterns and computational demands in modern cellular networks [4], [5], making efficient resource management a critical challenge. In this context, future communication systems must incorporate intelligent orchestration mechanisms to dynamically balance computation between network and device. This is especially important for XR applications, where device-level constraints play a central role: due to battery limitations and thermal effects, XR devices (e.g., visors) cannot sustain prolonged execution of complex workloads locally.

Thermal aspects are particularly critical due to the close contact between device and user skin: excessive heating may cause discomfort, reduce QoE through performance degradation [6], and in severe cases, even risk skin burns [1]. In this context, a promising solution is XR offloading, in which edge-based servers complement the device capabilities (e.g., computation) [7], [8]. As offloading is not free from concerns, including costs and networking issues like blockage and congestion [9], it is of primary importance to ponder when offloading is beneficial, i.e., when not doing so would result in battery or temperature issues [10].

Designing and supporting high-QoE XR experiences critically depends upon understanding and accurately modeling how device-level dynamics, namely power consumption, battery evolution, and temperature, evolve under workload. Indeed, while offloading decisions could rely only on instantaneous measurements (e.g., "offload to the edge if the temperature is above a certain threshold"), predicting the evolution of metrics such as temperature and battery level enables proactive management, resulting in better performance and user experience. For this reason, most studies [10], [11] rely on a *model* of XR devices. However, only few prior works derive and validate such models through real-world measurements, especially for current-generation XR hardware. Specifically, [12] focuses on performance evaluation of Meta's flagship VR hardware under Wi-Fi connectivity, while [13] explores energy profiling of VR applications across different usage domains. Neither work provides a compact, measurement-based model of XR

This work was supported by the innovation programme under Grand Agreement No. 101095363 and by the European Union under the Italian National Recovery and Resilience Plan of NextGenerationEU (PE00000001 – program "RESTART").

device dynamics or jointly captures power, battery, and thermal behavior.

We bridge the above gap, by conducting an extensive experimental campaign and showing that XR device behavior can be captured through compact linear equations. The models we derive not only allow for an easily interpretable mapping between the system parameters and clear understanding of their impact, but they also accurately represent power, battery, and temperature dynamics under realistic workloads, enabling lightweight prediction for QoE-aware offloading and resource management. The advantages of our approach and results are thus twofold. *First,* we demonstrate that XR device behavior can be modeled with tractable formulations, enabling scalable and real-time optimization. *Second,* our openly available dataset will facilitate reproducibility and foster further research, including the development of alternative models and QoE-driven XR system designs.

Our contributions can be summarized as follows:

- We conduct an extensive experimental campaign using real-world hardware and applications to explore the device-level dynamics that affect QoE (Sec. II);
- We propose a measurement-based model linking the key quantities governing XR device behavior, such as power consumption, battery level, and temperature, enabling the prediction of performance degradation that impacts QoE (Sec. III);
- We demonstrate how the proposed model can be used to predict operating limits under different workload and ambient conditions, highlighting battery- and thermal-driven constraints that affect sustained QoE (Sec. IV);
- We will release a publicly available dataset upon paper acceptance to support reproducibility and research on QoE-aware XR system design.

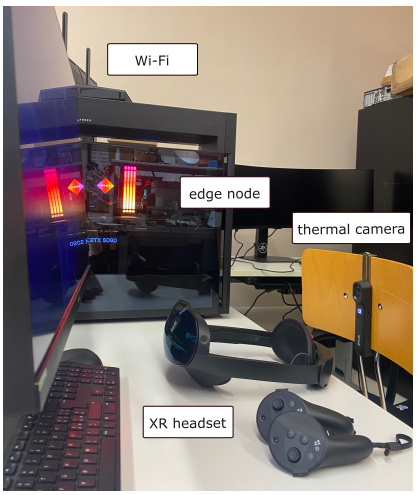
II. Experimental Analysis

This section first introduces our reference system and the XR testbed we developed (Sec. II-A), then it presents the experiments we performed and the obtained measurements (Sec. II-B), which are the foundation to derive our XR system model described later in Sec. III.

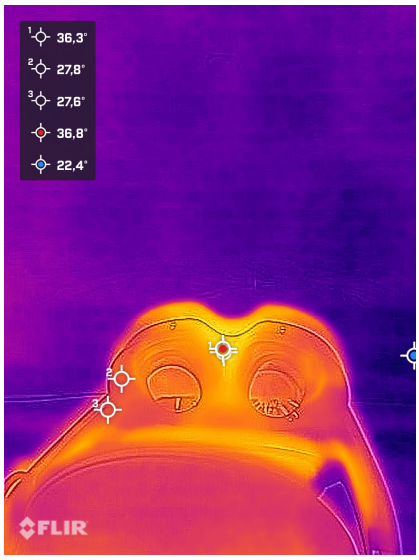
A. XR Testbed

We consider the XR system illustrated in Fig. 1(a), which comprises a wearable headset (i.e., Meta Quest Pro) and an edge computing node (i.e., a high-performance HP OMEN 45L GT22 gaming PC featuring an Intel Core Ultra 9 5.7 GHz processor, 64 GB RAM, and an NVIDIA GeForce RTX 5090 GPU with 32 GB of memory), interconnected via a wireless network (i.e., 5 GHz Wi-Fi). The setup also includes a FLIR Edge Pro thermal camera to measure the headset's external temperature [14], as shown in Fig. 1(b). In this scenario, device behavior directly affects the QoE perceived by users.

The workload consists of a $1080p$ video streaming application that combines real-time communication, high-definition video, and graphics processing, reflecting a typical multimedia XR session. Computationally intensive tasks, such as rendering and video encoding, are offloaded to the edge



(a) XR experimental setup



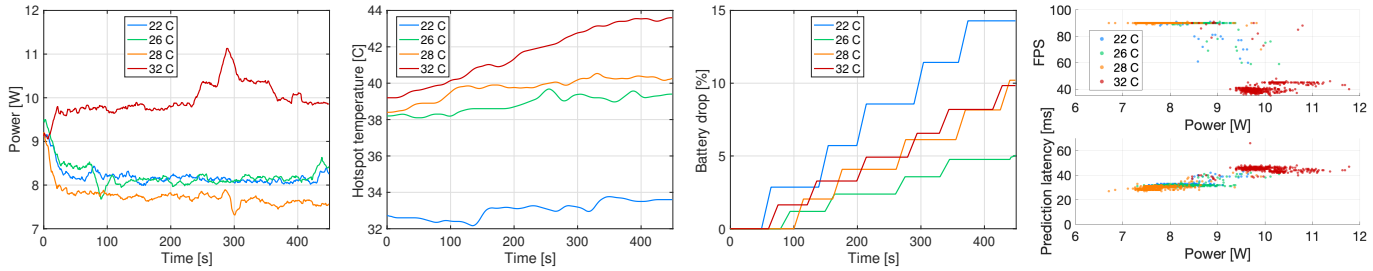
(b) Thermal image of headset

Fig. 1. Experimental setup and thermal characterization of XR device.

node, while the headset is responsible for video decoding, sensor tracking, and final display. This scenario represents a realistic multimedia XR workload that combines real-time wireless communication, high-definition video streaming, and graphics processing, while capturing interactions between edge computation and on-device resource utilization. Specifically, offloading reduces local computation but introduces sustained network activity, while the remaining on-device processing still generates significant thermal and energy load. As a result, power consumption, temperature evolution, and battery dynamics are tightly coupled and must be analyzed together.

B. Experimental Results

Building on the reference scenario and our testbed, we now analyze the measured behavior of the XR system. We collect both internal telemetry and external temperature measurements. The internal parameters include frame (FPS) rate, CPU/GPU utilization and frequency, power consumption, bat-



(a) Power (b) Hotspot temperature (c) Battery drop (d) QoE metrics

Fig. 2. Temporal evolution of key system-level metrics under different ambient temperatures (a-c), and relationship between power consumption and QoE-relevant application-level metrics (d).

tery level and temperature, and prediction latency[1]. External thermal measurements include hotspot temperature in the face-contact region, as shown in Fig. 1(b), and are particularly important as they capture the heat perceived by the user, linking device operation to user comfort, safety, and overall QoE. The experiments are conducted under four ambient temperatures: 22°C, 26°C, 28°C, and 32°C. Table I summarizes the overall impact of ambient temperature on key system metrics, while Fig. 2 illustrates the measured behavior of the XR headset under the four considered ambient temperatures. We first focus on the temporal evolution of the main system-level metrics, i.e., power consumption, external hotspot temperature, and battery drop, reported in Fig. 2(a)–(c).

Specifically, power consumption is shown in Fig. 2(a). The 32°C condition operates at higher and more variable power levels, approximately 9.5–11 W, indicating a more stressed operating regime. In contrast, the 22°C and 26°C cases remain stable around 8–8.5 W, while the 28°C case exhibits the lowest average power. A similar dependence on ambient temperature is observed for the external hotspot temperature in the nose-contact region, as shown in Fig. 2(b). As expected, higher ambient temperatures lead to elevated device temperatures throughout the session. The 32°C case exhibits the steepest increase, followed by 28°C, while 26°C and 22°C remain relatively stable. Initial temperature differences across trials are due to a brief preheating phase prior to the experiment.[2] Battery dynamics, reported in Fig. 2(c), show a step-like evolution and a non-monotonic dependence on ambient temperature. This suggests that battery depletion is determined not only by ambient temperature but also by device-level power management, workload scheduling, and thermal control mechanisms. The 22°C case experiences the largest drop, up to ≈14%, whereas 28°C and 32°C reach intermediate levels, around 10%. The 26°C scenario shows significantly lower depletion, below 6%, highlighting complex interactions among power management, thermal dynamics, and energy consumption.

[1]In the Meta Quest Pro telemetry, prediction latency represents the time needed by the XR pipeline to predict the headset pose and prepare the next frame for display, thus capturing the responsiveness of the application.

[2]All measurements were conducted without wearing the headset during the experiment to ensure user safety.

TABLE I
VALUES OF THE METRICS UNDER DIFFERENT AMBIENT TEMPERATURES

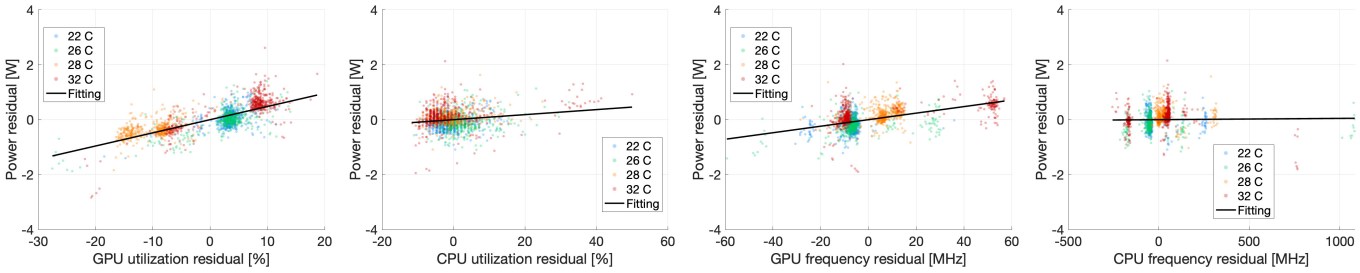
Notation	Metric	T_{amb} [°C]			
		22	**26**	**28**	**32**
CPU	Mean CPU utilization [%]	18.15	21.72	21.06	19.04
GPU	Mean GPU utilization [%]	78.47	77.82	63.99	97.17
f_{GPU}	Mean GPU frequency [MHz]	491.99	497.00	491.56	543.88
ΔT_{batt}	Battery temperature increase [°C]	1.0	1.0	1.0	4.0
ΔT	Hotspot temperature increase [°C]	1.0	1.5	2.3	4.4
ΔB	Battery drop rel. to start [%]	14.29	5.95	10.20	9.84
P	Mean power [W]	8.20	8.22	7.74	9.97
E	Cumulative energy [J]	$E(t) = \sum_i P_i \Delta t_i$			
-	Mean CPU level	2.02	2.04	2.01	4.90
-	Mean GPU level	3.05	3.18	3.03	4.28
-	Mean battery temperature [°C]	27.43	30.14	31.04	31.82
-	Hotspot initial temperature [°C]	32.1	38.1	38.0	39.2
-	Battery drop [% points]	5.00	5.00	5.00	6.00
-	Mean prediction latency [ms]	32.20	31.82	29.92	44.82
-	Mean FPS	89.47	89.52	89.94	42.40
-	Correlation $(GPU, \Delta T)$	-0.184	-0.292	-0.754	0.041
-	Correlation $(\Delta B, \Delta T)$	0.870	0.840	0.851	0.979
-	Correlation $(P, \Delta T)$	-0.221	-0.216	-0.473	0.487

Finally, Fig. 2(d) reports the impact of power consumption on application-level metrics directly related to QoE, i.e., FPS and prediction latency. Power consumption is relevant not only from an energy-efficiency perspective, but also as an indicator of workload intensity and thermal stress, both of which can affect application performance and QoE. At lower power levels, the system generally maintains high FPS and lower prediction latency. Conversely, under the 32°C condition, power consumption increases, and the application exhibits clear performance degradation, with FPS dropping to around 40-45 and prediction latency increasing to 45 ms.

Therefore, modeling how power consumption, hotspot temperature, and battery drop evolve during application execution is essential for characterizing XR device behavior and supporting QoE-aware prediction and control.

III. Analytical Modeling of the Relevant Performance Metrics

Building on the experimental analysis in Section II, we derive a compact analytical model of XR device behavior using the measured data. In particular, the trends observed in power consumption, hotspot temperature, and battery level evolution suggest that, within the considered operating regime,



(a) GPU utilization effect (b) CPU utilization effect (c) GPU frequency effect (d) CPU frequency effect

Fig. 3. Partial regression plots for the power model, showing the adjusted effect of each predictor after removing the contribution of the remaining predictors.

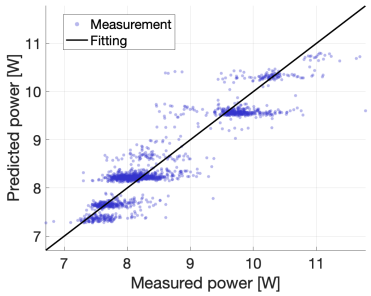


Fig. 4. Accuracy of the derived power model.

linear fitting provides an accurate and tractable approximation of the device dynamics. We therefore model the relationships among workload, power consumption, thermal evolution, and battery depletion using a set of linear equations.

To this end, we analyze each target metric as a function of the relevant system quantities. For each metric, we first discuss the measured dependencies observed through partial regression plots, then derive the corresponding analytical equation, and finally verify the fitting accuracy of the resulting model. The model coefficients are estimated from the experimental dataset using linear regression and are presented in Table II, along with the fitting error statistics.

Power. We first analyze power consumption. Fig. 3(a)-(d) shows how power varies with the considered workload-related quantities, namely GPU utilization, CPU utilization, GPU frequency, and CPU frequency. The partial regression plots highlight a linear dependence of power on the first three predictors, while the CPU frequency has a weaker effect. Based on these observations, we model power consumption as:

$$P{=}a_0{+}a_1 CPU{+}a_2 GPU{+}a_3 f_{GPU}{+}a_4 f_{CPU}, \qquad (1)$$

where P is the power consumption (W), CPU and GPU are the utilization levels (%), f_{GPU} and f_{CPU} are the GPU and CPU frequencies (MHz), and a_0, a_1, a_2, a_3, and a_4 are coefficients estimated through linear regression on the experimental measurements. The quality of the derived model is shown in Fig. 4, where measured and predicted power values are compared. The close alignment with the ideal fitting line confirms that the model accurately captures power consumption in the considered operating regime. Quantitatively, the power model achieves $R^2 = 0.87$, with an RMSE of 0.34 W. The fitting error reported in Table II remains limited, further confirming the accuracy of the linear model.

Temperature. We then analyze the external hotspot temperature increase, which is particularly relevant for user comfort, safety, and overall QoE. Fig. 5(a)–(c) shows the adjusted effect of cumulative energy, ambient temperature, and their interaction on the hotspot temperature increase. Thermal evolution is driven not only by cumulative energy but also by the surrounding thermal conditions. In particular, the positive trend in the interaction term suggests that the effect of energy accumulation strengthens at higher ambient temperatures. Based on these observations, we model the hotspot temperature increase as:

$$\Delta T{=}b_0{+}b_1 E_{\mathrm{kJ}}{+}b_2 T_{\mathrm{amb}}{+}b_3 E_{\mathrm{kJ}} T_{\mathrm{amb}}, \qquad (2)$$

where ΔT is the external hotspot temperature increase relative to the initial condition (°C), E_{kJ} is the cumulative energy consumption (kJ), T_{amb} is the ambient temperature (°C), and b_0, b_1, b_2, and b_3 are the model coefficients. The cumulative energy is computed as $E(t){=}\int_0^t P(\tau)\,d\tau$, which, in discrete time, is approximated as $E_k{=}\sum_{i=1}^{k} P_i \Delta t_i$, where k is the number of time slots we consider.

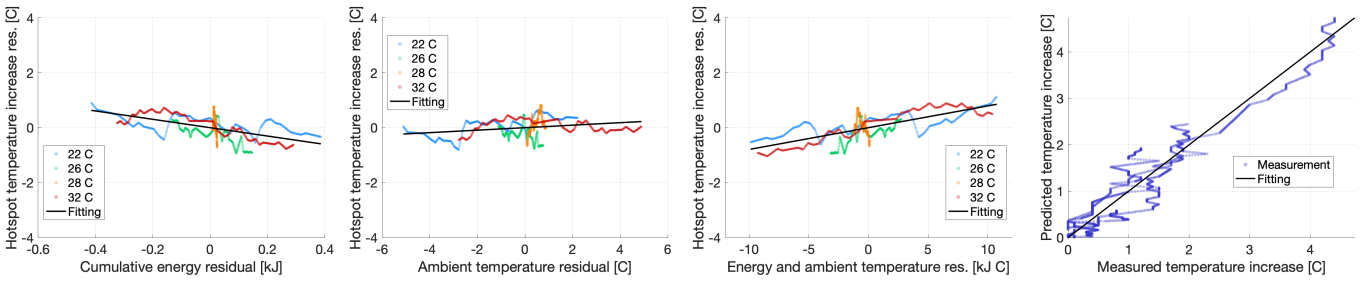
The quality of the derived model is shown in Fig. 5(d), achieving $R^2 = 0.93$, with an RMSE of 0.32°C, confirming the accuracy of the linear approximation.

Battery. Finally, we analyze battery drop, which directly affects the duration of an XR session. Fig. 6(a)-(c) shows how battery depletion varies with cumulative energy consumption, ambient temperature, and battery temperature increase. Battery drop is mainly driven by the energy spent during the session, while thermal conditions also contribute to the observed evolution. Based on these observations, we model battery drop as:

$$\Delta B(t){=}d_0{+}d_1 E(t){+}d_2 \Delta T_{\mathrm{batt}}(t){+}d_3 T_{\mathrm{amb}}, \qquad (3)$$

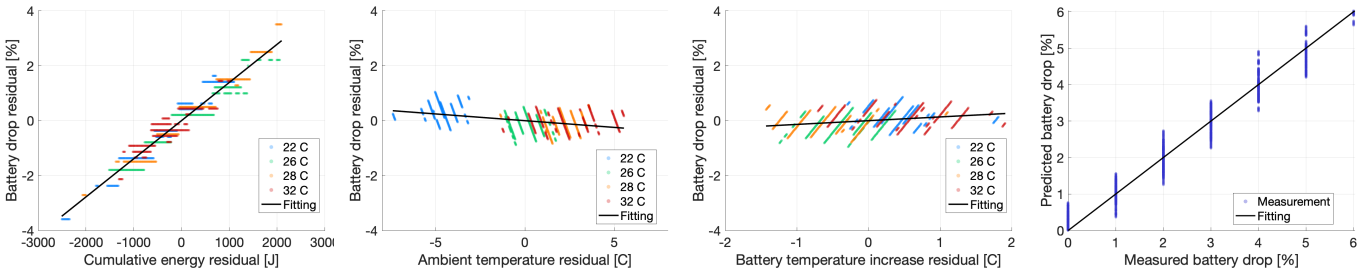
where $\Delta B(t)$ is the battery drop relative to the initial level, $E(t)$ is the cumulative energy consumption (J), $\Delta T_{\mathrm{batt}}(t)$ is the battery temperature increase with respect to its initial value (°C), T_{amb} is the ambient temperature (°C), and d_0, d_1, d_2, and d_3 are the model coefficients.

The quality of the derived model is shown in Fig. 6(d). The close agreement confirms that the model captures battery



(a) Cumulative energy effect (b) Ambient temperature effect (c) Both energy-temperature effect (d) Accuracy

Fig. 5. Partial regression plots for the hotspot temperature model, showing the adjusted effect of each predictor (a-c), and accuracy of the derived model (d).



(a) Cumulative energy effect (b) Ambient temperature effect (c) Battery temperature effect (d) Accuracy

Fig. 6. Partial regression plots for the battery model, showing the adjusted effect of each predictor (a-c), and accuracy of the derived model (d).

TABLE II
SUMMARY OF ANALYTICAL MODELS, ESTIMATED COEFFICIENTS, AND FITTING STATISTICS

Model	**Coefficients**	R^2	**RMSE**	**Var**
$P{=}a_0{+}a_1CPU{+}a_2GPU{+}a_3f_{GPU}{+}\ a_4f_{CPU}$	$a_0{=}-1.5,\ a_1{=}0.01,\ a_2{=}0.05,\ a_3{=}0.01\ a_4{\approx}0$	0.87	0.34 W	0.11
$\Delta T{=}b_0{+}b_1E_{\mathrm{kJ}}{+}b_2T_{\mathrm{amb}}{+}b_3E_{\mathrm{kJ}}T_{\mathrm{amb}}$	$b_0{=}-1.3,\ b_1{=}-1.5,\ b_2{=}0.05,\ b_3{=}0.08$	0.93	0.32°C	0.10
$\Delta B{=}d_0{+}d_1E{+}d_2\Delta T_{\mathrm{batt}}{+}d_3T_{\mathrm{amb}}$	$d_0{=}0.95,\ d_1{=}1.4{\times}10^{-3},\ d_2{=}0.14,\ d_3{=}-0.05$	0.97	0.34%	0.12

depletion during application execution. The battery model achieves $R^2 = 0.97$, with an RMSE of 0.34%.

Overall, the proposed model provides a compact representation of XR device dynamics by linking workload-dependent power consumption, cumulative energy, thermal evolution, and battery depletion. Although prior works assume more complex behaviors, such as exponential models [10], our results show that linear approximations are sufficient to accurately capture XR device dynamics within realistic operating ranges. This enables lightweight prediction of key device-level metrics during application execution, thereby supporting QoE-aware resource management and decision-making.

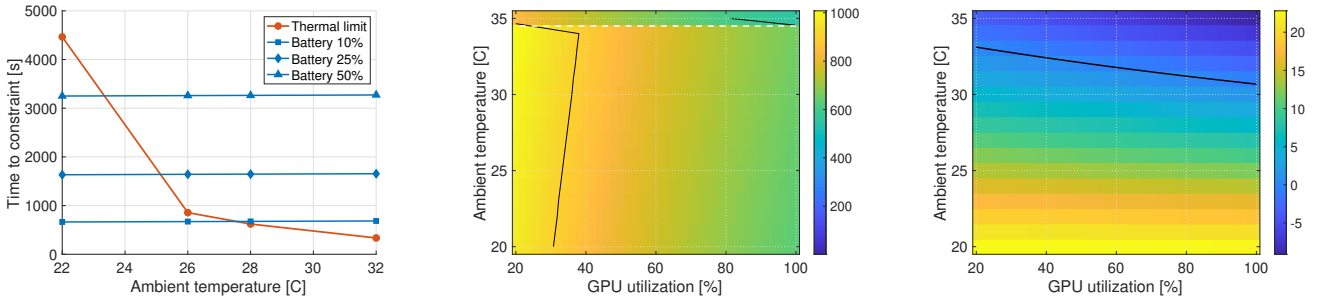
IV. Model Exploitation

This section shows how our model can be used to analyze the XR system behavior under prolonged operation to characterize its operating limits as a function of workload and ambient conditions.

We consider a *heavy workload* configuration, with CPU utilization of 70%, GPU utilization of 90%, and GPU frequency of 600 MHz. Under these conditions, the power model predicts a constant device power of 10 W. We evaluate two constraints: *(i)* a thermal safety limit corresponding to a maximum external hotspot temperature of 43°C [15], and *(ii)* battery-drop thresholds at different levels (10%, 25%, and 50%).

Fig. 7(a) shows the time required to reach the different operating limits as a function of ambient temperature. Battery-related constraints (10%, 25%, and 50% drop) remain nearly constant across ambient conditions. In contrast, the thermal limit exhibits a strong dependence on environmental conditions, decreasing sharply as ambient temperature increases. As a result, while battery constraints dominate at low ambient temperatures, thermal constraints quickly become the primary limiting factor at higher ambient temperatures, demonstrating the critical role of thermal management for sustained QoE.

Fig. 7(b) extends this analysis over a wider operating region by reporting the maximum safe session duration as a function of GPU utilization and ambient temperature. The color scale represents the time until the first constraint is violated. The black solid line denotes the boundary where the dominant constraint switches from battery-limited to thermal-limited operation. To the left of this boundary, the system is primarily limited by battery depletion, whereas to the right and at higher ambient temperatures, thermal constraints dominate. The white dashed line highlights the upper boundary of the feasible operating region. Safe operating time decreases with



(a) Time to reach thermal and battery limits (b) Maximum safe session duration (c) Thermal safety margin after session of 1200 s

Fig. 7. Model-based performance evaluation under heavy workload

both workload intensity and ambient temperature, and thermal effects increasingly constrain system operation as conditions become more demanding.

Finally, Fig. 7(c) presents the thermal safety margin as a function of GPU utilization and ambient temperature after a fixed session duration. The color scale indicates the distance from the thermal limit, and the black contour represents 43°C boundary. The margin decreases with both GPU utilization and ambient temperature. In particular, at elevated ambient temperatures, even moderate GPU utilization can drive the system beyond the thermal threshold. Compared to Fig. 7(b), this map provides an instantaneous view of thermal headroom, highlighting how close the system operates to its safety limit under different conditions.

V. Conclusions

Through an extensive experimental campaign, whose results will be publicly released upon paper acceptance as a Zenodo dataset to support reproducibility and further research, we have characterized XR device behavior under realistic operating conditions. Building on the real measurements, we have derived a compact, measurement-based linear model linking workload and environmental conditions to power consumption, battery dynamics, and thermal evolution. Despite the complexity of underlying processes, linear models provide an accurate representation of XR device dynamics within realistic operating regimes. This enables reliable prediction of system evolution over time, supporting efficient and lightweight optimization strategies.

Leveraging both model and experimental data, we have characterized XR system behavior under prolonged operation. Results reveal a clear separation of roles: battery sustainability is primarily driven by cumulative energy consumption, while thermal safety is strongly affected by ambient conditions and their interaction with workload intensity.

These insights highlight the need for adaptive and predictive system management strategies that jointly consider energy and thermal constraints. More importantly, they provide a foundation for QoE-aware XR system design, enabling an improved user experience by better controlling latency, performance stability, thermal comfort, and session duration.

References

[1] Ericsson., "Press release: Ericsson leads the 6G journey toward an intelligent fabric at MWC 2026." [Online] (accessed August 1, 2026) https://www.ericsson.com/en/press-releases/2026/3/ericsson-leads-the-6g-journey-toward-an-intelligent-fabric-at-mwc-2026https://www.ericsson.com/en/press-releases/2026, 2026.

[2] Fredrik Alriksson and Phillips, Chris and Pradas, Jose Luis and Zaidi, Ali and others, "XR and 5G: Extended Reality at Scale with Time-Critical Communication." [Online] (accessed August 1, 2026) https://www.ericsson.com/en/reports-and-papers/ericsson-technology-review/articles/xr-and-5g-extended-reality-at-scale-with-time-critical-communicationhttps://www.ericsson.com/en/reports-and-papers, 2021.

[3] R. Gu, J. Zhang, J. M. Rojas, and D. Shin, "On the promises and challenges of ai-powered xr glasses as embodied software," in *2025 2nd IEEE/ACM International Conference on AI-powered Software (AIware)*, pp. 207–212, IEEE, 2025.

[4] A. Boiano, N. Chukhno, Z. Smoreda, A. E. C. Redondi, M. Fiore, *et al.*, "A first look at operational ran updates and their impact on carrier traffic demands and prediction," in *IEEE International Conference on Computer Communications*, 2026.

[5] A. Boiano, M. Pirri, D. Madariaga, N. Chukhno, C. Ziemlicki, Z. Smoreda, A. E. C. Redondi, M. Fiore, *et al.*, "A longitudinal study of 5g nsa/sa infrastructure and user adoption from an mno perspective," in *IEEE International Conference on Computer Communications*, 2026.

[6] Y. S. K. Manjunath *et al.*, "Extended Reality Network Traffic & Quality of Experience." IEEE Dataport [Online] (accessed August 1, 2026) https://dx.doi.org/10.21227/na8a-9n63https://dx.doi.org/10.21227, 2025.

[7] O. Chukhno, N. Chukhno, A. Ometov, S. Pizzi, G. Araniti, and A. Molinaro, "Application-driven offloading of xr mission critical via integrated tn/ntn," *IEEE Network*, 2025.

[8] I. Yeregui, Á. Martín, M. Zorrilla, R. Viola, J. Astorga, and E. Jacob, "Towards context-aware edge-cloud continuum orchestration for multi-user xr services," *arXiv preprint arXiv:2602.03262*, 2026.

[9] E. Stafidas *et al.*, "A survey on enabling xr services in beyond 5g mobile networks," *IEEE Access*, 2024.

[10] F. Malandrino, O. Chukhno, A. Catania, A. Molinaro, and C. F. Chiasserini, "Xr offloading across multiple time scales: The roles of power, temperature, and energy," *IEEE Networking Letters*, 2025.

[11] O. Chukhno, F. Malandrino, A. Catania, A. Molinaro, and C. F. Chiasserini, "Enabling wearables towards the metaverse: Trade-offs involving blockage and heat," *IEEE Communications Magazine*, 2025.

[12] M. Jansen, J. Donkervliet, A. Trivedi, and A. Iosup, "Can my wifi handle the metaverse? a performance evaluation of meta's flagship virtual reality hardware," in *Companion of the 2023 ACM/SPEC international conference on performance engineering*, pp. 297–303, 2023.

[13] J. P. Kattakinda *et al.*, "Towards understanding the energy consumption of virtual reality applications in gaming, education, and entertainment," in *Proceedings of the ACM/IEEE 8th International Workshop on Games and Software Engineering*, pp. 50–57, 2024.

[14] FLIR, "Flir edge: Thermal camera with wireless connectivity for ios and android smart devices." [Online] (accessed August 1, 2026) https://www.flir.com/products/flir-edge/https://www.flir.com/products/.

[15] M. A. Rupp, "Is it getting hot in here? the effects of vr headset microclimate temperature on perceived thermal discomfort, vr sickness, and skin temperature," *Applied Ergonomics*, vol. 114, p. 104128, 2024.